THE JOURNAL OF PHYSICAL CHEMISTRY B

Article

pubs.acs.org/JPCB

Experimental Determination of Microsecond Reorientation Correlation Times in Protein Solutions

Enrico Ravera,[†] Giacomo Parigi,[†] Andi Mainz,[‡] Tomasz L. Religa,[§] Bernd Reif,[‡] and Claudio Luchinat*[,†]

[†]CERM, and Department of Chemistry "U. Schiff", University of Florence, Sesto Fiorentino, Italy

[‡]Technische Universitaet Muenchen, Dept. Chemie, Lichtenbergstrasse 4, D85747 Garching, Germany

[§]Department of Physiology and Biophysics, Case Western Reserve University, Cleveland, Ohio 44106, United States

ABSTRACT: Reorientation correlation times in protein solutions are key determinants for feasibility and quality of NMR experiments. Yet, their accurate estimate is not easy, especially in the case of very large proteins. We show that nuclear magnetic relaxation dispersion (NMRD) can accurately determine reorientation times up to the microsecond range. A theoretical description for the analysis of the NMRD profiles is provided, and the protein reorientation time is shown to be provided by the longest correlation time among those needed to reproduce the experimental profile. Measurements are performed using samples of the archaeal proteasome double ring $\alpha7\alpha7$ and of αB-Crystallin in glycerol solutions.

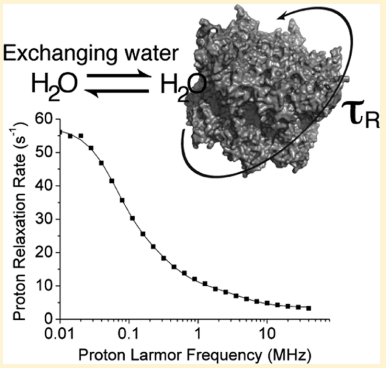

INTRODUCTION

In protein solutions, water protons are reporters of the reorientation motions of the protein: the longitudinal relaxation rates of water protons show a marked field dependence reflecting protein dynamics as a result of the interaction between water protons and the protein. Nuclear magnetic relaxation dispersions (NMRD),[1−9] measured by field cycling relaxometry,[10−13] yield spectral density functions that are superpositions of different motional processes, which in turn are associated with characteristic motional correlation times.[14−16] ^{1}H NMRD profiles are typically measured over a range of ^{1}H Larmor frequencies spanning from 0.01 to 50 MHz (and higher, using the most recent instrumentation[17] and/or high resolution NMR spectrometers). This means that correlation times spanning from 10^{-6} to 10^{-9} s can be accessible, i.e., information on the motions occurring in proteins from few kDa up to MDa can be obtained. Direct measurement of protein proton spectral density functions is also possible by dissolving proteins in D_2O and collectively monitoring the protein protons themselves.[18−20]

Determining the rotational correlation times through NMRD can be very useful for several reasons:

1. Monitoring of protein aggregation.
2. Optimization of protein solution conditions affecting protein tumbling (possible detection of faster motions[21] or observation of solid-like signals[22−26]).
3. As no labeling is required, NMRD permits to obtain information on the system before production of labeled samples.[27−29]

NMRD measurements can be easily performed with protein concentrations on the order of 0.1 mM for MW of about 500 kDa and on the order of 1 mM for MW of about 50 kDa. Aggregation at these protein concentrations would be evidenced, if present, by the occurrence of an unexpectedly large reorientation time. In the present study we show examples where the reorientation correlation times of systems as large as 600 kDa (human αB-Crystallin) in 20% v/v glycerol and 360 kDa ($\alpha7\alpha7$ proteasome from *Thermoplasma acidophilum*) in 40% v/v glycerol can be experimentally accessed.

EXPERIMENTAL METHODS

NMRD profiles were acquired using a high sensitivity fast field-cycling relaxometer (Stelar, Mede, Italy) at different temperatures in glycerol/water mixtures. ^{1}H longitudinal relaxation rates were extracted by single exponential fitting of magnetization decay or magnetization build-up curves at ^{1}H Larmor frequencies ranging from 0.01 to 40 MHz. The magnetization curve for water and glycerol protons have been treated as a single exponential function, because as previously shown,[30,31] water and glycerol protons relax with similar times. The time constant so obtained is equal within few percent to the average of the time constants of the two types of protons, so that the error introduced by the presence of glycerol is on the order of the experimental error of the data, up to a glycerol concentration of about 40%.

Sample conditions were 3.6 mM monomer concentration in 25 mM phosphate, pH 6.8, 50 mM NaCl, 1 mM EDTA, 0.03% NaN_3, 40% v/v glycerol for $\alpha7\alpha7$ proteasome, and 5.0 mM monomer concentration in 70 mM phosphate, pH 7.5, 70 mM

Received: December 20, 2012
Revised: February 14, 2013
Published: March 11, 2013

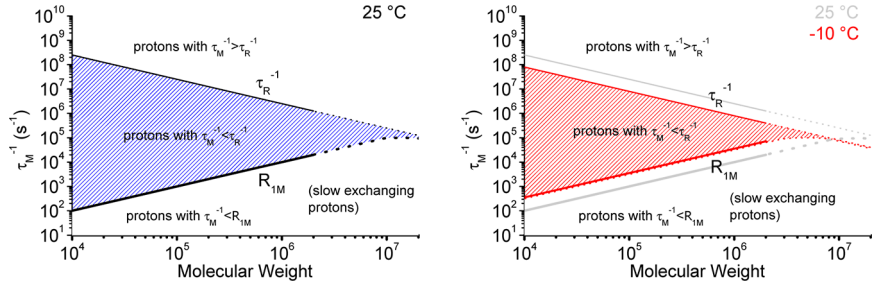

Figure 1. Proton exchange rate (τ_M^{-1}) is compared to the reorientation rate (τ_R^{-1}) and to the low field relaxation rate of water protons dipole−dipole coupled with correlation time τ_R to protein protons (R_{1M}) as a function of the protein MW, at 25 °C (black lines) and −10 °C (red lines).

NaCl, 20% v/v glycerol for αB-Crystallin. Proteins were prepared as described in refs 32,33 for α7α7 proteasome and in refs 34,35 for αB-Crystallin.

THEORETICAL BACKGROUND

Experimental water proton R_1 values in protein solutions are mainly ascribed to exchange between the bulk water protons and the protons that interact transiently with the protein itself. These transiently interacting protons are of three types:[15,36−38] The first type consists of exchangeable protein protons (e.g., backbone NHs and side chain NH or OH protons). The second type is represented by protons of water molecules that are bound to the protein as such. A third small contribution to R_1 arises from water molecules that interact with the protein so weakly that their dipole−dipole interactions are best described as being modulated by their diffusion nearby the protein. The correlation time modulating the dipole−dipole interactions of each water proton—or exchangeable protein proton—in the bound state is dominated by the shortest time among the reorientation time τ_R of the protein and the lifetime of the coupled protons τ_{Mi}:

$$\tau_i^{-1} = \tau_R^{-1} + \tau_{Mi}^{-1} \tag{1}$$

The resulting R_1 is determined by the sum of all contributions arising from each coupled nucleus, or pool of nuclei sharing common exchange properties (*vide infra*), according to the equation[3,15,37−39]

$$R_1 = \sum_i f_i \left[\frac{1}{R_{1Mi}} + \tau_{Mi}\right]^{-1} + a = \sum_i f_i \left[\frac{1}{\beta_i^2(0.2J(\omega, \tau_i) + 0.8J(2\omega, \tau_i))} + \tau_{Mi}\right]^{-1} + a \tag{2}$$

where f_i represents the molar fraction of the interacting protons with correlation time τ_i with respect to the bulk water protons, and β_i is a constant related to the dipole−dipole interaction energy. The nondispersive term a accounts for the protons with dipolar interactions modulated by diffusion nearby the protein.

The contribution to R_1 of each exchangeable protein proton or protein-bound water proton can be quite different depending on its lifetime τ_{Mi} with respect to the reorientation time of the protein and the R_{1Mi} value. Figure 1 shows the proton relaxation rates together with the protein reorientation rate as a function of the protein MW and of the proton lifetime. A first pool of protons is constituted by fast exchanging protons with $\tau_{Mi}^{-1} > \tau_R^{-1}$ (proton exchange is faster than the reorientation rate): the correlation time modulating the dipole−dipole interaction is in this case smaller than the protein reorientation time, and thus they do not bear information on τ_R. A second pool is defined for fast exchanging protons with $R_{1Mi} < \tau_{Mi}^{-1} < \tau_R^{-1}$: the nuclear relaxation of these protons is described by Lorentzian dispersions with correlation time provided by the protein reorientation time. These are the protons bearing information on τ_R. The third pool of protons contains slowly exchanging protons, with $\tau_{Mi}^{-1} < R_{1Mi}$. The correlation time of the Lorentzian dispersions is again τ_R, but since R_1 is limited by the τ_{Mi} term in eq 2, which becomes dominant, the dispersion is quenched by the long proton lifetime. Therefore, the dispersion appears distorted, seemingly shifted to higher fields, and thus yielding a smaller apparent correlation time (unless the value of τ_{Mi} is properly taken into account).

The population of the three pools depends on the protein reorientation time, and thus on the protein MW and on sample conditions like viscosity, temperature, and pH. Figure 1 provides a graphical representation of the range of conditions that define the behavior of the three pools of protons. By increasing MW, the protein reorientation time increases. Consequently, the low fields R_{1M} of protons with correlation time τ_R increases. Therefore, the range of the exchange rates that protons must have to bear direct information on the reorientation time of the protein is reduced. Analogously, the interval of proton exchange rates providing direct information on τ_R is reduced by decreasing temperature, again because the protein reorientation time increases together with the low fields R_{1M}.

Exchangeable protein protons can have very different exchange rates depending on pH, up to few thousands of s^{-1}.[39−41] When MW is so large that $R_{1M} \cong \tau_R^{-1}$ (dotted lines in Figure 1), the spin-relaxation exceeds the Redfield limit,[42,43] and R_{1M} stops increasing linearly with MW. In fact, the relaxation time can never be as short as the correlation time of the interaction causing relaxation, because it is not conceivable that a modulation can induce a change in a physical property (the orientation of a spin) at a rate higher than the modulation rate itself. In the assumption underlying the Redfield limit, this would mean that the energy of the dipole−dipole coupling, whose modulation is responsible for relaxation, must be smaller than the inverse of the correlation time for the modulation of the coupling itself. Out of the Redfield limit, this does not mean that the interaction energy cannot be larger than τ_R^{-1}: if the dipole−dipole coupling energy is increased in a system within the Redfield limit, R_{1M} increases initially proportionally to the square of the energy, and then more and more slowly as R_{1M} approaches τ_R^{-1}, until a limiting value of the order of τ_R^{-1} is reached.[43,44]

Possible local motions further complicate the picture. In fact, the presence of these fast motions, with correlation times τ_{fi},

dx.doi.org/10.1021/jp312561f | J. Phys. Chem. B 2013, 117, 3548−3553

introduces additional spectral density functions to R_{1Mi} with local correlation times given by

$$\tau_i^{-1} = \tau_R^{-1} + \tau_{fi}^{-1} + \tau_{Mi}^{-1}$$

The analysis of the experimental data can be simplified by assuming that the profiles can be reproduced by the sum of Lorentzian dispersions, corresponding to different τ_i values.[14,45] An average correlation time $\langle\tau_c\rangle$ can be defined as the weighted average of the best fit correlation times.[14,45] For small proteins it was shown that $\langle\tau_c\rangle$ is in good agreement with the reorientation time as calculated from the Stokes' equation. However, it was already noted that this does not hold for large systems like apoferritin.[14] This was initially ascribed to the presence of different aggregation states, apoferritin being a polymer composed of 24 subunits.

RESULTS AND DISCUSSION

The ^{1}H relaxation profiles of αB-Crystallin in 20% (v/v) glycerol at 25, −3, and −10 °C, and the α7α7 proteasome in 40% (v/v) glycerol at 25, −5, and −15 °C are reported in Figures 2 and 3, respectively. The profiles have been fitted to

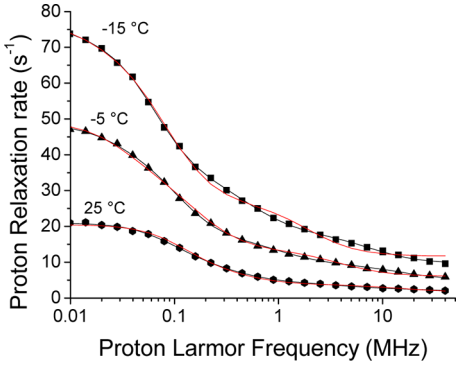

Figure 2. Water proton relaxation rates for the 95 mg/mL α7α7 proteasome solution at −15, −5, and 25 °C. The lines represent the best fit profiles (see text).

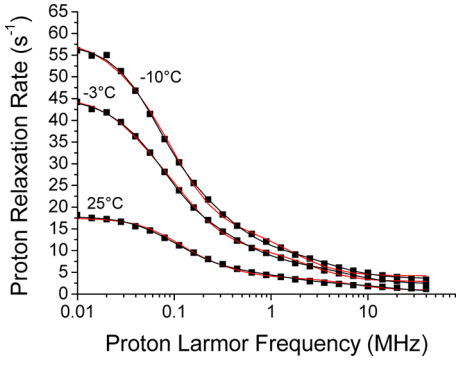

Figure 3. Water proton relaxation rates for the 100 mg/mL αB-Crystallin solution at −10, −3, and 25 °C. The lines represent the best fit profiles (see text).

the sum of Lorentzian dispersions, corresponding to different τ_i values. Initially all protons were assumed in the fast exchange regime, i.e., with lifetime τ_M much shorter than their relaxation time, so that τ_M can be neglected in eq 2. The profiles were fitted using three correlation times, according to the following equation:

$$R_1 = a + b_{1fe}[0.2J(\omega, \tau_1) + 0.8J(2\omega, \tau_1)] + b_2[0.2J(\omega, \tau_2) + 0.8J(2\omega, \tau_2)] + b_3[0.2J(\omega, \tau_3) + 0.8J(2\omega, \tau_3)]$$

where $b_i = f_i\beta_i$, and the a term accounts for the contributions by protons with very short lifetime, the dispersion of which occurs beyond the highest accessible magnetic field, besides containing the contribution of diffusing water molecules. In the absence of protein aggregation, the correlation time τ_1 is thus expected to be equal to τ_R, due to long-lived water molecules (i.e., with $\tau_M > \tau_R$) and exchangeable protein protons whose dipole−dipole interactions are modulated by the protein reorientation time, i.e., again with $\tau_M > \tau_R$.

In order to reduce the covariance among the unknown parameters (a, b_{1fe}, b_2, b_3, τ_1, τ_2, τ_3) used to fit the experimental data to eq 3, the profiles of αB-Crystallin at 25, −3, and −10 °C were fit simultaneously. Also the profiles of the α7α7 proteasome at 25, −5, and −15 °C were fit simultaneously. The ratios between the τ_i values for the different temperatures, $\delta\tau$, was kept constant in the three dispersions, and fixed to the values calculated from the ratios between the different reorientation times. Such reorientation times were estimated with hydroNMR,[46] and resulted in 1.5, 4.3, and 6.1 μs at 25, −3, and −10 °C, respectively, for αB-Crystallin in 20% glycerol; $\delta\tau^{-3}$ ($= \tau^{-3}/\tau^{25}$) was thus fixed to 2.8 and $\delta\tau^{-10}$ ($= \tau^{-10}/\tau^{25}$) to 4.0. For α7α7 proteasome, reorientation times of 0.90, 3.6, and 7.2 μs at 25, −5, and −15 °C, respectively, in 40% glycerol, were estimated with hydroNMR,[46] so that $\delta\tau^{-5}$ ($= \tau^{-5}/\tau^{25}$) and $\delta\tau^{-15}$ ($= \tau^{-15}/\tau^{25}$) could be fixed to 4.0 and 8.0, respectively. The sum of the b_i parameters ($b_{tot} = b_{1fe} + b_2 + b_3$) was constrained to be the same for the three temperatures.

These fits, showed as red lines in Figures 2 and 3 are relatively good for αB-Crystallin but not satisfactory for the α7α7 proteasome at the lowest temperature. The best fit parameters are reported in Tables 1 and 2.

In order to improve the quality of the fits, two additional minimizations were performed:

1. A fourth correlation time was included in the fit.
2. A fraction of protons with the largest correlation time was allowed to be in the slow exchange regime. In this case, the profiles were fitted according to the following equation:

$$R_1 = a + b_{1se}\left[\frac{1}{0.2J(\omega, \tau_1) + 0.8J(2\omega, \tau_1)} + k_M\right]^{-1} + b_{1fe}[0.2J(\omega, \tau_1) + 0.8J(2\omega, \tau_1)] + b_2[0.2J(\omega, \tau_2) + 0.8J(2\omega, \tau_2)] + b_3[0.2J(\omega, \tau_3) + 0.8J(2\omega, \tau_3)] \quad (3)$$

where $k_M = \beta_1\tau_M$ and the indices se and fe stand for slow exchange and fast exchange ($b_{tot} = b_{1se} + b_{1fe} + b_2 + b_3$).

The quality of both these minimizations is very good for both proteins (Figures 2 and 3 and Tables 1 and 2). In the first minimization, the longest correlation time is 1.16 μs for αB-Crystallin and 0.76 μs for the α7α7 proteasome. The corresponding weights are somewhat smaller than the values calculated from the minimization with three correlation times.

In the second minimization, k_M is indeed limiting the dispersion of most of the protons with correlation time τ_1. The fit indicates that the fast exchanging protons with the largest

dx.doi.org/10.1021/jp312561f | J. Phys. Chem. B 2013, 117, 3548−3553

Table 1. Best Fit Parameters for the 95 mg/mL α7α7 Proteasome Solution[a]

residuals=		35.11 (red fit)	6.60	4.57 (black fit)
a^{25}	s^{-1}	1.74	1.42	1.34
a^{-5}	s^{-1}	6.06	5.32	4.99
a^{-15}	s^{-1}	11.74	10.03	9.69
b_{tot}	s^{-2}	3.49×10^8	7.11×10^8	8.98×10^8
$b_{1fe}{}^{25}/b_{tot}$		6.2%	2.5%	1.7%
$b_{1se}{}^{25}/b_{tot}$				7.9%
$b_2{}^{25}/b_{tot}$		5.3%	2.5%	10.3%
$b_3{}^{25}/b_{tot}$		88.5%	13.2%	80.1%
$b_4{}^{25}/b_{tot}$			81.81%	
$b_{1fe}{}^{-5}/b_{tot}$		1.7%	0.6%	0.3%
$b_{1se}{}^{-5}/b_{tot}$				10.8%
$b_2{}^{-5}/b_{tot}$		10.9%	4.7%	9.6%
$b_3{}^{-5}/b_{tot}$		87.4%	10.1%	79.3%
$b_4{}^{-5}/b_{tot}$			84.7%	
$b_{1fe}{}^{-15}/b_{tot}$		0.5%	0.1%	0.1%
$b_{1se}{}^{-15}/b_{tot}$				13.0%
$b_2{}^{-15}/b_{tot}$		11.2%	4.2%	10.4%
$b_3{}^{-15}/b_{tot}$		88.3%	13.0%	76.6%
$b_4{}^{-15}/b_{tot}$			82.69%	
$\tau_1{}^{25}$ (= τ_R at 25 °C)	s	6.66×10^{-7}	7.64×10^{-7}	8.59×10^{-7}
$\tau_2{}^{25}$	s	1.34×10^{-7}	1.68×10^{-7}	1.94×10^{-8}
$\tau_3{}^{25}$	s	5.81×10^{-9}	1.78×10^{-8}	1.45×10^{-9}
$\tau_4{}^{25}$			1.65×10^{-9}	
$k_M{}^{25}$	s^{-1}			1.76×10^7
$k_M{}^{-5}$	s^{-1}			3.59×10^6
$k_M{}^{-15}$	s^{-1}			2.78×10^6
$\delta\tau^{-5}$	*Fixed to* 4.0			
$\delta\tau^{-15}$	*Fixed to* 8.0			

[a]The parameters are labelled with 25, −5, and −15 to indicate the values at 25, −5, and −15 °C, respectively. The indices fe and se indicate fast exchange and slow exchange, respectively.

Table 2. Best Fit Parameters for the 100 mg/mL αB-Crystallin Solution[a]

residuals=		16.75 (red fit)	6.11	5.96 (black fit)
a^{25}	s^{-1}	0.85	0.69	0.56
a^{-3}	s^{-1}	2.87	2.41	2.43
a^{-10}	s^{-1}	4.18	3.46	3.58
b_{tot}	s^{-2}	2.36×10^8	3.80×10^8	4.06×10^8
$b_{1fe}{}^{25}/b_{tot}$		5.9%	2.0%	1.1%
$b_{1se}{}^{25}/b_{tot}$				8.0%
$b_2{}^{25}/b_{tot}$		4.7%	4.2%	10.2%
$b_3{}^{25}/b_{tot}$		89.4%	11.8%	80.7%
$b_4{}^{25}/b_{tot}$			81.96%	
$b_{1fe}{}^{-3}/b_{tot}$		2.9%	0.8%	0.3%
$b_{1se}{}^{-3}/b_{tot}$				17.0%
$b_2{}^{-3}/b_{tot}$		13.4%	7.2%	12.0%
$b_3{}^{-3}/b_{tot}$		83.7%	14.5%	70.6%
$b_4{}^{-3}/b_{tot}$			77.6%	
$b_{1fe}{}^{-10}/b_{tot}$		1.3%	0.2%	0.0%
$b_{1se}{}^{-10}/b_{tot}$				18.9%
$b_2{}^{-10}/b_{tot}$		16.3%	7.4%	13.9%
$b_3{}^{-10}/b_{tot}$		82.5%	17.1%	67.2%
$b_4{}^{-10}/b_{tot}$			75.28%	
$\tau_1{}^{25}$ (= τ_R at 25 °C)	s	8.18×10^{-7}	1.16×10^{-6}	1.42×10^{-6}
$\tau_2{}^{25}$	s	2.23×10^{-7}	3.11×10^{-7}	6.01×10^{-8}
$\tau_3{}^{25}$	s	1.31×10^{-8}	4.16×10^{-8}	5.43×10^{-9}
$\tau_4{}^{25}$			4.52×10^{-9}	
$k_M{}^{25}$	s^{-1}			4.08×10^6
$k_M{}^{-3}$	s^{-1}			2.47×10^6
$k_M{}^{-10}$	s^{-1}			2.02×10^6
$\delta\tau^{-3}$	*Fixed to* 2.8			
$\delta\tau^{-10}$	*Fixed to* 4.0			

[a]The parameters are labelled with 25, −3, and −10 to indicate the values at 25, −3, and −10 °C, respectively. The indices fe and se indicate fast exchange and slow exchange, respectively.

correlation time represent a minor component and that the corresponding molar fraction decreases with decreasing temperature, whereas the molar fraction of slow exchanging protons (the major component of protons with the largest correlation time) increases. The fits provide lifetimes at lower temperatures which are smaller than those at higher temperatures. Because an increase in the exchange rate with decreasing temperature is not possible for a given proton, the fits suggest that the average τ_M value is determined by different fractions of protons at the three temperatures. Actually, the largest contribution to relaxation is determined by protons with $\tau_M{}^{-1}$ on the order of or larger than R_{1M} (see Figure 1), the corresponding dispersions being increasingly quenched for decreasing proton exchange rates. Since R_{1M} increases with decreasing temperature, also the best-fit $\tau_M{}^{-1}$ increases, because a different fraction of protons with larger $\tau_M{}^{-1}$ provides the largest contribution to relaxation.

For the α7α7 proteasome in 40% v/v glycerol, the fraction of protons with largest correlation time, which amounts to 0.86, 3.4, and 6.9 μs at 25, −5, and −15 °C, respectively, corresponds to 9.6%, 11.1%, and 13.1% at the three temperatures (see Table 3); for αB-Crystallin in 20% v/v glycerol, the fraction of protons with largest correlation time, found equal to 1.4, 4.0, and 5.7 μs at 25, −3, and −10 °C, respectively, corresponds to 9.1%, 17.3%, and 18.9% at the same temperatures (Table 3).

Table 3. Best Fit Protein Reorientation Times (τ_R) and Fraction of Protons with These Correlation Times

protein	temperature	τ_R (μs)	fraction
α7α7 proteasome (40% glycerol)	25 °C	0.86	9.6%
	−5 °C	3.4	11.1%
	−15 °C	6.9	13.1%
αB-Crystallin (20% glycerol)	25 °C	1.4	9.1%
	−3 °C	4.0	17.3%
	−10 °C	5.7	18.9%

This fraction increases with decreasing temperature, probably due to the increased R_{1M} value (see Figure 1).

If a fourth correlation time is included into eq 3, the quality of the fit does not improve significantly, and the analysis of the results is complicated by the increased covariance among the fitting parameters.

For both proteins, the largest correlation times obtained through these two minimizations are quite similar, around 15% and 20% larger when the presence of slow exchanging protons is considered, for the α7α7 proteasome and for αB-Crystallin, respectively. This indicates that the longest correlation times are well determined.

Differently from what observed for small proteins, as already noted for apoferritin, also for proteasome and αB-Crystallin the average correlation time $\langle\tau_c\rangle$, defined as the weighted average of the best fit correlation times,[14,45] is not in agreement with the

dx.doi.org/10.1021/jp312561f | J. Phys. Chem. B 2013, 117, 3548−3553

reorientation time as calculated from the Stokes' equation or hydroNMR calculations. The latter time rather corresponds to the largest correlation time obtained in the fit. This different behavior can be ascribed to larger contributions of fast local motions and exchange to the correlation time modulating the dipole−dipole interaction, as the result of the increased τ_R (see eq 1).

In order to understand why $\langle\tau_c\rangle$ does not agree with the expected reorientation time of the protein, we can refer to Figure 1 to monitor how the relaxation rate of water protons which are dipole−dipole coupled to protein protons changes with increasing MW. As seen before, fast exchanging protons providing a full dispersion with correlation time τ_R are those with $R_{1M} < \tau_M^{-1} < \tau_R^{-1}$. It can be easily appreciated from Figure 1 that the number of these protons decreases sizably with increasing MW of the protein. The number of protons with $R_{1M} < \tau_M^{-1} < \tau_R^{-1}$ is further reduced by decreasing temperature (and/or increasing viscosity). Only these protons actually provide information on the reorientation time τ_R. Therefore, only the Lorentzian dispersion with largest correlation time acts as a reporter for the protein tumbling time.

This holds in the assumption that there is no protein aggregation, which can be in any case detected through the concentration dependence of the relaxation profiles. From the analysis of the correlation times obtained from the relaxation profiles at different protein concentration it has been in fact possible to monitor the presence of aggregation phenomena in several proteins.[14,19,47,48] A good fit of all profiles under the assumption of no aggregation at any temperature, and the obtained reorientation times in good agreement with expectations and measurements through dynamic light scattering,[34] ensures that in the present systems aggregation is absent or rather limited.

In the presence of protein anisotropy, the accessible largest correlation time is expected to be the average (harmonic mean) reorientation time. For the present proteins, anisotropy is not very pronounced, as also confirmed by the hydroNMR calculations.

CONCLUSIONS

We have examined the theory underlying proton relaxation in solutions containing large proteins: the use of an average $\langle\tau_c\rangle$ for estimating the reorientation time of the macromolecules in solution, that was proven correct for small proteins, does not give satisfactory results in the case of large systems, whose rotational diffusion is better represented by the largest τ alone. The reorientation times of the investigated proteins can be determined from the analysis of the NMRD profiles, and found to be as large as 0.9 and 1.4 μs for the $\alpha7\alpha7$ proteasome in 40% v/v glycerol and αB-Crystallin in 20% v/v glycerol, respectively at 25 °C, in good agreement with the hydroNMR prediction and the hydrodynamic radius of αB-Crystallin calculated through dynamic light scattering measurements.[34] The analysis indicates that (i) the longest correlation time τ_1, related to the lowest field dispersion, is the one that is sensitive to τ_R; and (ii) the exchange time of a relatively important fraction of protons is limiting the observed relaxation effect. The protons with correlation time τ_1 are below 10% at 25 °C and below 20% at the lowest temperature for both samples.

AUTHOR INFORMATION

Corresponding Author

*Tel. +390554574262. Fax +390554574253. E-mail: claudioluchinat@cerm.unifi.it.

Notes

The authors declare no competing financial interest.

ACKNOWLEDGMENTS

This work has been supported by Ente Cassa di Risparmio di Firenze, MIUR-FIRB contract RBFR08WGXT, PRIN 2009FAKHZT, and the European Commission, contract Bio-NMR no. 261863 and Instruct, part of the European Strategy Forum on Research Infrastructures (ESFRI) and supported by national member subscriptions. Specifically, we thank the EU ESFRI Instruct Core Centre CERM, Italy.

REFERENCES

(1) Koenig, S. H.; Schillinger, W. E. *J. Biol. Chem.* **1969**, *244*, 3283−3280.
(2) Koenig, S. H.; Brown, R. D., III *Prog. NMR Spectrosc.* **1990**, *22*, 487−567.
(3) Bertini, I.; Luchinat, C.; Parigi, G. *Solution NMR of paramagnetic molecules*; Elsevier: Amsterdam, 2001.
(4) Halle, B.; Denisov, V. P. *Methods Enzymol.* **2001**, *338*, 178−201.
(5) Kroes, S. J.; Salgado, J.; Parigi, G.; Luchinat, C.; Canters, G. W. *J. Biol. Inorg. Chem.* **1996**, *1*, 551−559.
(6) Luchinat, C.; Parigi, G. *Appl. Magn. Reson.* **2008**, *34*, 379−392.
(7) Bertini, I.; Luchinat, C.; Parigi, G. *Adv. Inorg. Chem.* **2005**, *57*, 105−172.
(8) Nusser, W.; Kimmich, R. *J. Phys. Chem.* **1990**, *94*, 5637−5639.
(9) Korb, J.-P.; Bryant, R. G. *J. Chem. Phys.* **2001**, *115*, 10964−10974.
(10) Noack, F. *Prog. NMR Spectrosc.* **1986**, *18*, 171−276.
(11) Koenig, S. H.; Brown, R. D., III *NMR Spectroscopy of Cells and Organisms*; CRC Press: Boca Raton, 1987; Vol. *II*, p 75.
(12) Kimmich, R.; Anoardo, E. *Prog. NMR Spectrosc.* **2004**, *44*, 257−320.
(13) Ferrante, G.; Sykora, S. *Adv. Inorg. Chem.* **2005**, *57*, 405−470.
(14) Bertini, I.; Fragai, M.; Luchinat, C.; Parigi, G. *Magn. Reson. Chem.* **2000**, *38*, 543−550.
(15) Venu, K.; Denisov, V. P.; Halle, B. *J. Am. Chem. Soc.* **1997**, *119*, 3122−3134.
(16) Halle, B.; Denisov, V. P.; Venu, K. *Biol. Magn. Reson.* **1999**, *17*, 419−483.
(17) High field relaxometer, Stelar s.r.l.: Mede, Italy, www.stelar.it.
(18) Bertini, I.; Gupta, Y. K.; Luchinat, C.; Parigi, G.; Schlörb, C.; Schwalbe, H. *Angew. Chem., Int. Ed.* **2005**, *44*, 2223−2225.
(19) Luchinat, C.; Parigi, G. *J. Am. Chem. Soc.* **2007**, *129*, 1055−1064.
(20) Borsi, V.; Luchinat, C.; Parigi, G. *Biophys. J.* **2009**, *97*, 1765−1771.
(21) Ban, D.; Gossert, A. D.; Giller, K.; Becker, S.; Griesinger, C.; Lee, D. *J. Magn. Reson.* **2012**, *221*, 1−4.
(22) Goddard, Y. A.; Korb, J.-P.; Bryant, R. G. *J. Magn. Reson.* **2009**, *199*, 68−74.
(23) Bertini, I.; Luchinat, C.; Parigi, G.; Ravera, E.; Reif, B.; Turano, P. *Proc. Natl. Acad. Sci. U.S.A.* **2011**, *108*, 10396−10399.
(24) (a) Bertini, I.; Engelke, F.; Luchinat, C.; Parigi, G.; Ravera, E.; Rosa, C.; Turano, P. *Phys. Chem. Chem. Phys.* **2012**, *14*, 439−447. (b) Bertini, I.; Luchinat, C.; Parigi, G.; Ravera, E. *Acc. Chem. Res.* **2013**, DOI: 10.1021/ar300342f.
(25) Bertini, I.; Engelke, F.; Gonnelli, L.; Knott, B.; Luchinat, C.; Osen, D.; Ravera, E. *J. Biomol. NMR* **2012**, *54*, 123−127.
(26) Gardiennet, C.; Schütz, A. K.; Hunkeler, A.; Kunert, B.; Terradot, L.; Böckmann, A.; Meier, B. H. *Angew. Chem. Int. Ed.* **2012**, *51*, 7855−7858.
(27) Pervushin, K. V.; Wider, G.; Riek, R.; Wüthrich, K. *Proc. Natl. Acad. Sci. U.S.A.* **1999**, *96*, 9607−9612.

(28) Matzapetakis, M.; Turano, P.; Theil, E. C.; Bertini, I. *J. Biomol. NMR* **2007**, *38*, 237−242.
(29) Tugarinov, V.; Hwang, P. M.; Ollerenshaw, J. E.; Kay, L. E. *J. Am. Chem. Soc.* **2003**, *125*, 10420−10428.
(30) Bertini, I.; Luchinat, C.; Xia, Z. *J. Magn. Reson.* **1992**, *99*, 235−246.
(31) Bertini, I.; Capozzi, F.; Luchinat, C.; Xia, Z. *J. Phys. Chem.* **1993**, *97*, 1134−1137.
(32) Tugarinov, V.; Sprangers, R.; Kay, L. E. *J. Am. Chem. Soc.* **2007**, *129*, 1743−1750.
(33) Religa, T. L.; Sprangers, R.; Kay, L. E. *Science* **2010**, *328*, 98−102.
(34) Mainz, A.; Jehle, S.; van Rossum, B. J.; Oschkinat, H.; Reif, B. *J. Am. Chem. Soc.* **2009**, *131*, 15968−15969.
(35) Mainz, A.; Bardiaux, B.; Kuppler, F.; Multhaup, G.; Felli, I. C.; Pierattelli, R.; Reif, B. *J. Biol. Chem.* **2012**, *287*, 1128−1138.
(36) Hills, B. P. *Mol. Phys.* **1992**, *76*, 489−508.
(37) Kiihne, S.; Bryant, R. G. *Biophys. J.* **2000**, *78*, 2163−2169.
(38) Denisov, V. P.; Halle, B. *Faraday Discuss.* **1996**, *103*, 227−244.
(39) Libralesso, E.; Nerinovski, K.; Parigi, G.; Turano, P. *Biochem. Biophys. Res. Commun.* **2005**, *328*, 633−639.
(40) Liepinsh, E.; Otting, G. *Magn. Reson. Med.* **1996**, *35*, 30−42.
(41) Banci, L.; Berners-Price, S.; Bertini, I.; Clementi, V.; Luchinat, C.; Spyroulias, G. A.; Turano, P. *Mol. Phys.* **1998**, *95*, 797−808.
(42) Redfield, A. G. *Adv. Magn. Reson.* **1965**, *1*, 1−32.
(43) Kowalewski, J.; Luchinat, C.; Nilsson, T.; Parigi, G. *J. Phys. Chem. A* **2002**, *106*, 7376−7382.
(44) Bertini, I.; Luchinat, C.; Kowalewski, J. *J. Magn. Reson.* **1985**, *62*, 235−241.
(45) Halle, B.; Jóhannesson, H.; Venu, K. *J. Magn. Reson.* **1998**, *135*, 1−13.
(46) de la Torre, J. G.; Huertas, M. L.; Carrasco, B. *J. Magn. Reson.* **2000**, *147*, 138−146.
(47) Berti, F.; Costantino, P.; Fragai, M.; Luchinat, C. *Biophys. J.* **2004**, *86*, 3−9.
(48) Koenig, S. H.; Brown, R. D., III; Spiller, M.; Chakrabarti, B.; Pande, A. *Biophys. J.* **1992**, *61*, 776−785.